catalysts

MDPI

Review

Conversion of CO_2 into Glycolic Acid: A Review of Main Steps and Future Challenges

Marcelo Tavares Lima [1], Nouridine Ousseini Salifou [2], George Victor Brigagão [3], Ivaldo Itabaiana, Jr. [1] and Robert Wojcieszak [2,*]

[1] Department of Biochemical Engineering, School of Chemistry, Federal University of Rio de Janeiro, Rio de Janeiro 21941-910, Brazil; marcelotl@eq.ufrj.br (M.T.L.); ivaldo@eq.ufrj.br (I.I.J.)
[2] Univ. Lille, CNRS, Centrale Lille, Univ. Artois, UMR 8181—UCCS—Unité de Catalyse et Chimie du Solide, F-59000 Lille, France; nouridinesalifou27@gmail.com
[3] Polytechnic School, Federal University of Rio de Janeiro, Rio de Janeiro 21941-909, Brazil; george.victor@poli.ufrj.br
* Correspondence: robert.wojcieszak@univ-lille.fr; Tel.: +33-(0)320-336-708

Abstract: Exploring the potential of utilizing CO_2 for commercial purposes is a promising opportunity, especially in light of the growing research efforts towards CO_2 capture, storage, and utilization as well as green H_2 production. This review article delves into catalyst features and other technological aspects of a plausible process for the indirect conversion of CO_2 into glycolic acid, which involves the following steps: CO_2 capture, water electrolysis, CO_2 hydrogenation to methanol, catalytic oxidation to formaldehyde, and formaldehyde carbonylation to glycolic acid. We adopt an industrial perspective to address this challenge effectively, thoroughly evaluating different processing alternatives with emphasis on the catalytic systems to optimize glycolic acid production performance.

Keywords: glycolic acid; CO_2 capture; green hydrogen; CO_2 hydrogenation; methanol oxidation; formaldehyde carbonylation

Citation: Tavares Lima, M.; Salifou, N.O.; Brigagão, G.V.; Itabaiana, I., Jr.; Wojcieszak, R. Conversion of CO_2 into Glycolic Acid: A Review of Main Steps and Future Challenges. *Catalysts* **2024**, *14*, 4. https://doi.org/10.3390/catal14010004

Academic Editor: Giuseppe Bonura

Received: 30 November 2023
Revised: 16 December 2023
Accepted: 17 December 2023
Published: 19 December 2023

1. Introduction

To achieve the goals of the Paris Agreement, global anthropogenic CO_2 emissions should be zero by 2050, and although major CO_2 sources come from power, steel, and cement industries [1,2], efforts from all areas of society will be needed. However, the challenge involves unequal abatement costs across sectors. For example, chemical and steel companies may face higher costs for decarbonization in comparison with electricity generation plants [3]. In this scenario, carbon capture and storage (CCS) and carbon capture and utilization (CCU) are solutions for CO_2 abatement that are widely discussed in the literature [4–6]. Both involve separation processes to avoid the release of CO_2 to the atmosphere, generated by conversion of fossil or biomass resources, differing mainly by fate of the CO_2 stream and whether it contributes to revenues of the project.

CCS prescribes sending captured CO_2 (e.g., from combustion, industrial separation, or direct air capture) to geological storage, returning carbon to underground locations if it comes from a fossil resource. Power plants with CCS have been extensively studied in the literature [7] regarding challenges in the efficient capture and safe storage of CO_2 [8]. CCS can provide considerable reduction of global CO_2 emissions by 2050 [9,10], but the deployment of projects depends on a combination of favorable local aspects and leverages, like regulatory requirements and proper economic incentives [11].

In turn, CCU encompasses all routes where CO_2 is used commercially to add revenues, either chemically as a raw material or physically as in enhanced oil recovery (EOR), among other uses. The concept may be regarded as a current "hot topic", but it is not new. Back in 1972, a plant was launched in Texas for the purpose of improving productivity of old wells by EOR using CO_2 captured from natural gas. Most early projects addressed EOR and

utilized CO_2 that had to be captured for other reasons (e.g., natural gas conditioning), but even in the 1970s there were studies considering the capture of CO_2 from flue gases, which is believed by some as the origin of the CCS/CCU concept [8]. The chemical conversion of CO_2 has also been studied for many decades [11], as a possible low-cost raw material, with possible uses in the production of methanol and methane by hydrogenation, as well as in carboxylation reactions to produce carbonates, acrylates, and polymers [12,13]. However, since CO_2 is a relatively stable molecule, the processes are usually energy-intensive. Also, the reaction kinetics for CO_2 conversion require special catalysts [14].

Beyond global warming concerns related to energy use and direct CO_2 emissions, other significant environmental problems are caused by non-biodegradable plastic waste. It is well known to impact ecosystems but may also indirectly lead to the emission of greenhouse gases (e.g., from landfilling and incineration) [14–16]. This kind of waste mostly consists of common synthetic polymers like polyolefins (polyethylene, polypropylene), polyethylene terephthalate (PET), and nylon, as well as their combinations and composites. In this scenario, one sustainable alternative is to invest in the production of biodegradable polymers like polyglycolic acid (PGA), whose monomer (glycolic acid) can be produced from renewable feedstocks (Figure 1), showing reduced lifetime (i.e., better biodegradability) when compared to other sustainable polymers (e.g., polycaprolactone and polybutylene adipate-co-terephthalate) [15].

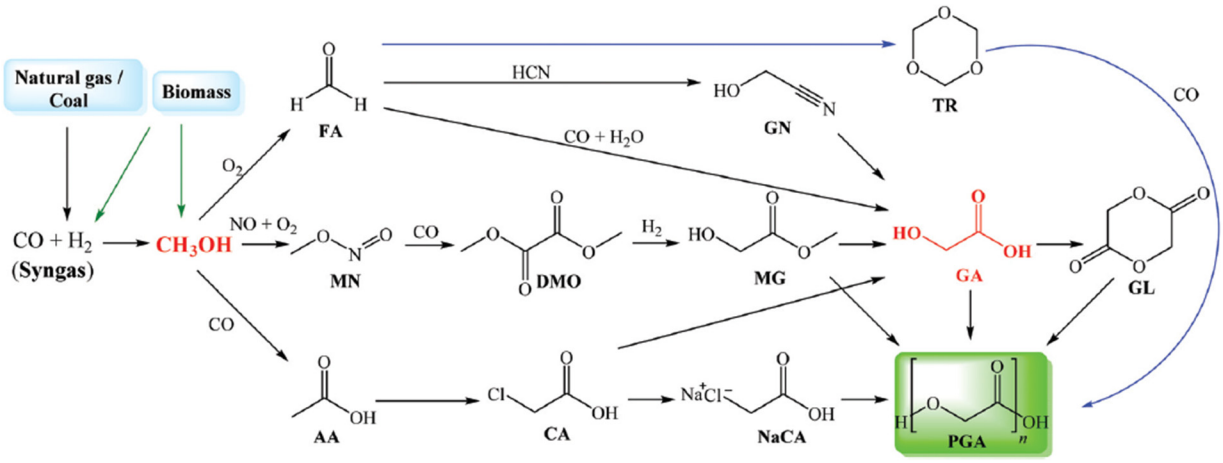

Figure 1. Reaction pathways from syngas to polyglycolic acid polymers.

Glycolic acid also has other applications, and its global demand has increased, with possible use in food, cosmetic, textile, and cleaning chemical industries [17–19]. The production of glycolic acid from CO_2 involves the following sequence of steps: syngas generation (e.g., by gasification), CO_2 and/or CO separation (excess CO_2 can be geologically stored), methanol synthesis, methanol partial oxidation, and formaldehyde reaction with CO (carbonylation). In this short review we detail each process step from a technical perspective, emphasizing the achievements and outcomes of each stage. Given that catalysts play a pivotal role in facilitating the various reactions, a comparative strategy is embraced to pinpoint the best catalysts based on yield and catalytic activity considerations.

2. CO_2 Capture

The production of polyglycolic acid can be carried out through different reaction pathways, shown in Figure 1. The routes have in common the need for methanol synthesis, where hydrogen reacts with CO and CO_2. In this case, a CCU concept could be employed to replace syngas production, with CO_2 hydrogenation to methanol addressed by use of renewable H_2 from electrolysis. The CO_2 could be obtained through different capture technologies, with the choice being mainly a function of the characteristics of the gas carrying the CO_2 to be captured and the energy resource of the process; in a general way, the lower the CO_2 partial pressure and the carbon content of the resource gas, the more

expensive the capture process. The capture strategies are generally classified into three main groups when applied to power generation processes: pre-combustion, post-combustion, and oxy-combustion [20,21]. They are briefly described below.

In pre-combustion CO_2 capture, the fuel (e.g., biomass, coal, natural gas) is firstly converted into syngas and then subjected to shift conversion to react CO and increase H_2 content, as illustrated in Figure 2. Syngas generation occurs between 700 and 1000 °C, and the required heat is usually supplied in situ by partial oxidation or indirectly by combustion. Then, H_2/CO_2 fractionation takes place, usually by chemical or physical absorption, and the H_2 stream experiences combustion. The advantage of the strategy relies mainly in performing separation with relatively high CO_2 fugacity, in comparison with typical flue gases of the post-combustion route. The major drawback is the high capital investment, which is a consequence of the much greater plant complexity [22,23].

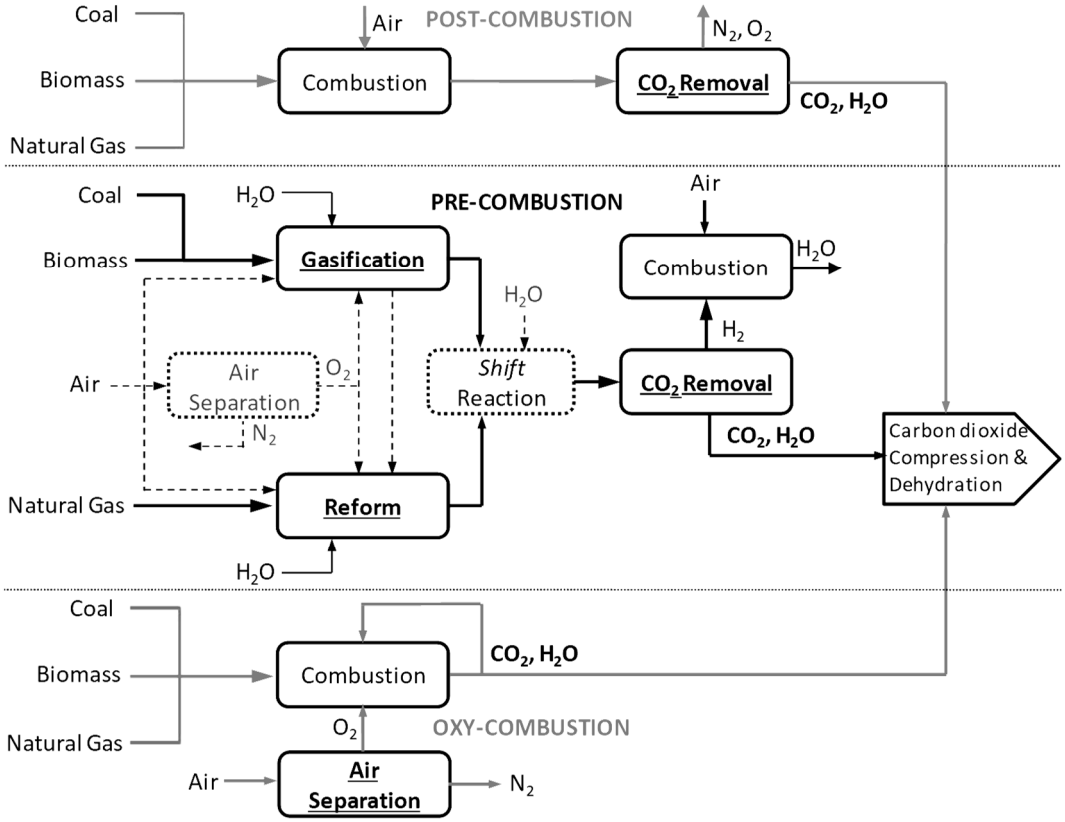

Figure 2. Overview of main conceptual routes for CO_2 capture in power generation processes.

Post-combustion CO_2 capture concept consists of removing CO_2 from flue gas (Figure 2). This method is particularly advantageous when the CO_2 content is relatively low [24,25]. The concept allows easy CCS adaptation to various industrial and power settings, requiring minimum change in the original plant. In this case, chemical absorption with aqueous alkanolamines is a mature solution for this separation service, readily available for commercial implementation [26]. The technology is well known for its use in natural gas processing, with more than 6 decades of application [20]. The main drawback is the high operating cost linked to CO_2 removal in low fugacity from a low-pressure N_2-rich stream. Absorption processes are sensitive to the presence of NOx and SOx and require a solvent makeup to compensate for losses from volatilization, inactivation, or degradation [23].

The process of oxy-combustion (Figure 2) involves burning fuel with pure oxygen instead of air to minimize nitrogen introduction to the system, resulting in exhausts primarily composed of CO_2 + H_2O, which has the advantage of dismissing a separation process for CO_2 removal in exchange for a process for oxygen production. The economic competitive-

ness of this concept is thus highly dependent on air separation performance [27], which usually entails high power demand and high capital investment [28].

The various possible technologies for CO_2 separation can be categorized into five generic groups (Figure 3): absorption, adsorption, membrane permeation, cryogenic distillation, and chemical looping combustion (CLC) [24]. Chemical absorption with amines is the most mature technology, given the experience of decades of large-scale plant operation. These chemical solvents have high reactivity with CO_2, relatively high thermal stability, and high absorption capacity. The major drawback is the relatively high heating demand for solvent regeneration [20]. Post-combustion capture by such amines in a thermal power station involves a countercurrent contact of the gas with the solvent in a packed column operated at nearly atmospheric pressure and a temperature of 40–70 °C [25]. Some substances commonly used for this purpose are monoethanolamine (MEA), methyl-diethanolamine (MDEA), and 2-amino-2-methyl-1-propanol (AMP) [29,30]. The mechanism involved in CO_2 chemical absorption by MEA is shown in Equations (1) and (2). Its regeneration heat, expressed by mass of captured CO_2, is nearly 4 $GJ/ton_{(CO2)}$ if it is applied to mitigate emissions from a natural gas power plant. An alternative to minimize heating demand is to employ phase change solvents [31], e.g., by addition of an alcohol to MEA, which allows reduction of the amount of solvent to be regenerated, thus decreasing the heating demand associated with CO_2 capture. The general flowsheet of a standard chemical absorption plant for CO_2 removal is shown in Figure 4 [32]. Besides chemical absorption, physical absorption is also mature and commercially available (e.g., SELEXOL, RECTISOL, NMP PURISOL), being applicable when the stream is pressurized and when CO_2 has enough fugacity. Physical solvents are less selective—implying lower CO_2 purity—but can be regenerated at lower temperatures by stream depressurization.

$$MEA + CO_2 + H_2O \rightarrow MEACOO^- + H_3O^+ \quad (1)$$

$$MEACOO^- + H_3O^+ \rightarrow MEA + CO_2 + H_2O \quad (2)$$

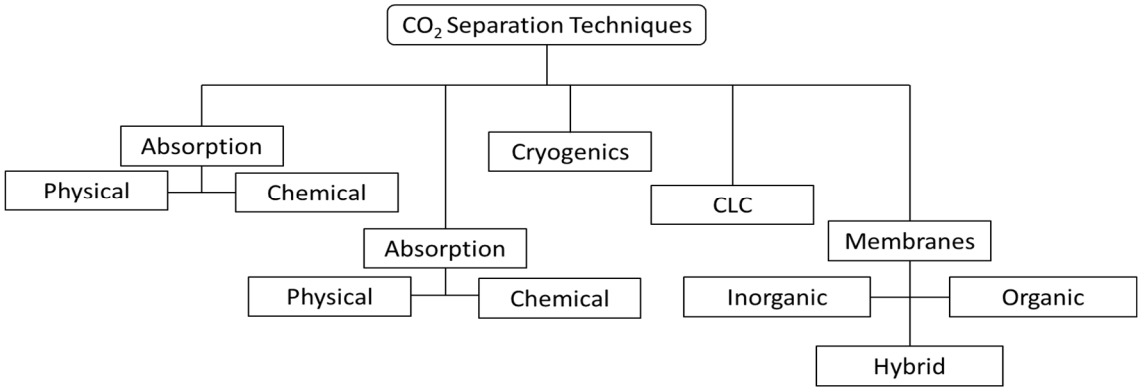

Figure 3. Technologies applied for CO_2 separation process. Reprinted with permission from [30].

Separation by adsorption can occur through physical (e.g., using zeolites, activated carbon, or metal-organic frameworks) or chemical mechanisms (e.g., metal oxides, hydrotalcites, lithium zirconate) [33], among which physical adsorption has been more frequently used for CO_2 capture. It involves a selective interaction between the target adsorbate CO_2 and a solid material, which retains the CO_2 in its surface, to later be regenerated, usually by pressure or temperature variation. At least two vessels installed in parallel are required for continuous cyclic operation: while one tower is regenerated, another one is active in the process. The cycle duration depends on adsorbent capacity and regeneration method (it usually operates for a few hours without regeneration if it is temperature-swing, but only a few minutes if it is pressure-swing) [34].

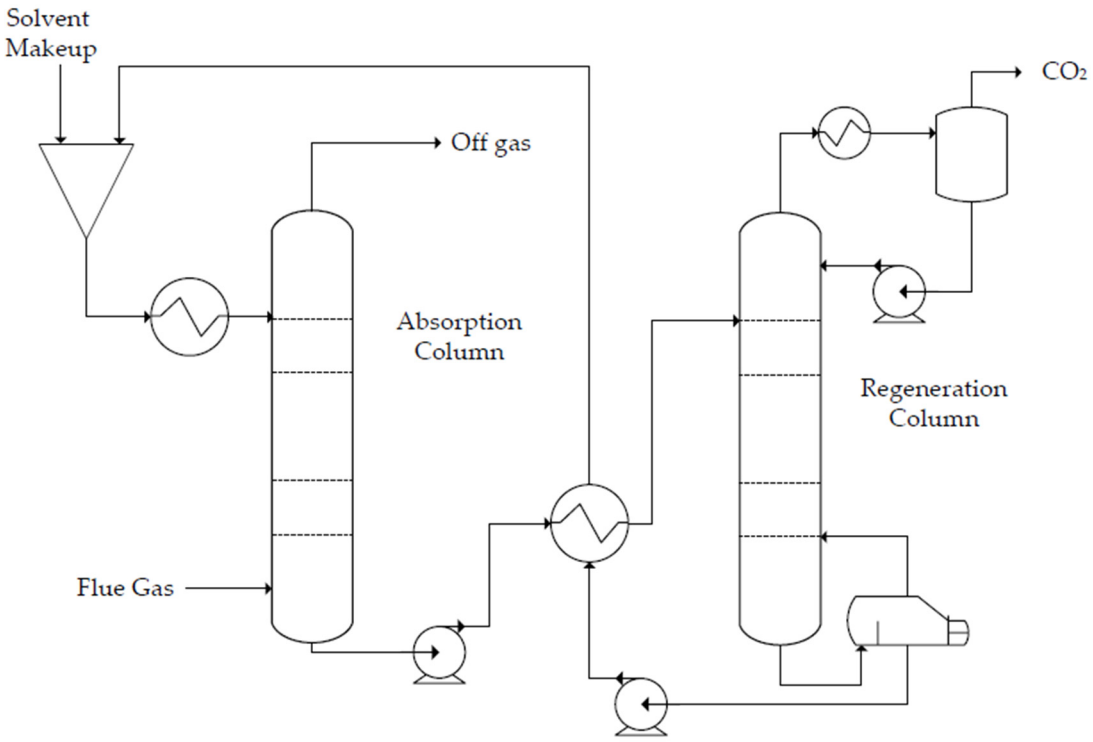

Figure 4. Typical flowsheet of CO_2 chemical absorption by amine-based solvent. Adapted from [32].

A relatively new concept is the use of selective membranes to separate CO_2 from a gas stream. Membranes are semipermeable barriers that can be manufactured using different materials, which can be an organic (e.g., polymer) or inorganic type (e.g., ceramic, metallic). Separation by polymeric membranes has been more relevant in the field, and it is already utilized commercially for natural gas processing, since the stream is already found at high pressure, where it offers significant advantages of operational flexibility. The following two perspectives are important in the evaluation of membrane performance: permeability (for certain pressure drop) and selectivity (permeability ratio) of desired components. These determine component recoveries and stream purities after the separation process. The main drawbacks of gas permeation are low scalability (it is manufactured in modules), low product purity, and the need to compress the feed stream to generate separation driving-force if it is received at low pressure, which generally makes the option economically unattractive when compared to other separation methods [25]. In addition, the material may be sensitive to the presence of certain contaminants in the gas (e.g., sulfur compounds). However, membranes can be advantageous to promote process intensification in reactors and to improve reaction performance by in situ separation, as discussed in later sections [25].

Another separation method is cryogenic distillation, which is capable of producing high-purity streams and CO_2 already pressurized and liquefied, ready to be pumped for transportation. The process involves high capital investment (due to feed gas pretreatment, large amount of involved equipment, and requirement of resistant material for low-temperature operation) and high operating costs (linked to refrigeration), being economically competitive in large-scale applications where the feed stream has high CO_2 content (usually above 50%) [22]. Some further advantages of this process—besides the production of pure liquid CO_2—are the absence of solvents and good scalability (economic performance is substantially improved by process scale-up). Some of the existing process designs differ in how CO_2 freeze-out is avoided or managed (CO_2 solidification may be allowed at certain conditions, depending on the process) [22,35].

Chemical-looping combustion (CLC) uses metal oxides as oxygen carriers to convert the fuel and generate heat, in order to produce CO_2 + H_2O flue gas as in oxy-combustion

(it is often classified in this category). A cyclic process of oxidation with air and reduction with fuel takes place to avoid the direct contact of air and fuel. The concept efficiently promotes CO_2 capture with low energy requirements, while avoiding the presence of N_2 in the flue gas, which not only increases the CO_2 content but also has the further advantage of avoiding the formation of NO_x. Besides high oxidation/reduction activity, the material should present long-term stability, with good mechanical resistance and minimum agglomeration. Additionally, the material should enable complete oxidation of the fuel for maximum system efficiency. Oxygen carriers meeting these requirements are under development [36].

3. Hydrogen Production Unit

Methanol plants require syngas generation or pure H_2 production for CO_2 hydrogenation. To avoid CO_2 emissions, and also to allow chemical conversion of captured CO_2, renewable electricity from wind farms and/or solar energy can be used—promoting integration of clean technologies into a broader energy landscape—to produce pure H_2 (up to 99.99%v) from water electrolysis [37], which occurs through the reactions shown in Equations (3)–(5) [38]. Water electrolysis can be carried out through different methods, which include alkaline water electrolysis, proton exchange membranes, anion exchange membranes (AEMs), and solid oxide electrolysis, among others. Table 1 compares different electrolysis systems according to their operating conditions, technological status, and advantages and disadvantages [39].

$$\text{anode } H_2O \rightarrow \frac{1}{2}O_2 + 2H^+ + 2e^- \quad (3)$$

$$\text{cathode } 2H^+ + 2e^- \rightarrow H_2 \quad (4)$$

Generally speaking, the electrolysis of water releases hydrogen and oxygen:

$$H_2O \rightarrow H_2 + \frac{1}{2}O_2 \quad (5)$$

Table 1. Classification and characteristics of the different hydrogen production technologies for electrolysis. Adapted with permission from [39].

Category	Alkaline Electrolysis	Proton Exchange Membrane	Proton Exchange Membrane	Solid Oxide Electrolysis	Solid Oxide Electrolysis	Solid Oxide Electrolysis
Charge carrier	OH^-	OH^-	H^+	H^+	O^{2-}	O^{2-}
Temperature	20–80 °C	20–200 °C	20–200 °C	500–1000 °C	500–1000 °C	750–900 °C
Electrolyte	Liquid	Solid Polymer			Solid Ceramic	
Anode	Ni > Co > Fe; perovskite; $LaCoO_3$	Ni	IrO_2, RuO_2, $Ir_xRu_{1-x}O_2/TiO_2$, TiC	Perovskite	$La_xSr_{1-x}MnO_3$ + Y-ZrO_2 (LSM-YSZ)	$La_xSr_{1-x}MnO_3$ + Y-ZrO_2 (LSM-YSZ)
Cathode	Ni alloys	Ni, Ni-Fe, $NiFe_2O_4$	Pt/C MoS_2	Ni	Ni-YSZ $LaCrO_3$	Ni-YSZ Perovskite
Efficiency	59–70%	-	65–82%	100%	100%	-
TRL *	9	4–5	6–7	3–5	3	3–5
Advantages	Low investment cost, stable, well-known technology	Combination of alkaline and membrane electrolysis	Compact technology, very high H_2 purity	Strengthening of kinetics and thermodynamics, low energy demand, low investment cost		
Disadvantages	Corrosive electrolyte, very slow dynamics	Low conductivity of OH- in polymers	High cost of membrane polymers, requires noble metals	Mechanical instability of the electrodes, safety problems, poor sealing		

* TRL = Technology readiness level.

Alkaline electrolysis is usually carried out at 20–80 °C using nickel as the electrocatalyst and water mixed with strong hydroxide (e.g., NaOH, KOH) to produce H_2 99%v. The system is already commercially available but has the drawbacks of slow start-up and the requirement of a constant power supply. Proton exchange membrane-type electrolysis is a promising alternative for widespread deployment, as it can provide a faster response with greater process efficiency, though it involves more capital investment due to expensive membranes and electrocatalysts. The amount of hydrogen produced is a function of the current intensity (the relationship is given by Faraday's Law of Electrolysis). Solid oxide electrolysis requires lower voltages and is capable of much greater performance due to lower power demand. A drawback is that it requires operation at temperatures well above 500 °C, which also has shown to shorten the lifetime of the ceramic membranes. This technology is not yet commercially available for large-scale application [39].

4. CO_2 Hydrogenation to Methanol

Methanol synthesis is an exothermic catalytic process usually addressed in gas-phase conditions, using syngas with H_2 excess over a catalyst fixed bed at ≈250 °C and 50–100 bar. In the case of hydrogenation of pure CO_2, some changes are commonly introduced in the catalyst, but the involved chemical reactions are practically the same. The reaction of CO_2 hydrogenation is presented in Equation (6), which occurs with incomplete conversion due to limitations of chemical equilibrium. In parallel, CO formation also takes place by reverse water–gas shift, a competitive reaction also limited by equilibrium, which is represented by Equation (7). The low single-pass conversion of reactants is usually circumvented by recycling at least 90% of the unconverted gas, which enhances overall carbon efficiency. The typical flowsheet of the synthesis loop is shown in Figure 5 [40]. Carbon monoxide is believed by some as also susceptible to direct conversion to methanol, following the reaction shown in Equation (8); however, there is experimental evidence from tests with carbon isotope 14 in syngas indicating that the CO has to be converted to CO_2 prior to methanol formation [41,42]. Nevertheless, kinetic modelling of methanol synthesis has been approached in the literature regarding diverse hypothetical mechanisms. In this sense, kinetic models applicable for CO_2 hydrogenation over commercial methanol catalysts can be found in recent studies [43].

$$CO_2 + 3H_2 \rightleftharpoons CH_3OH + H_2O \quad (6)$$

$$CO_2 + H_2 \rightleftharpoons CO + H_2O \quad (7)$$

$$CO + 2H_2 \rightleftharpoons CH_3OH \quad (8)$$

Methanol formation equilibrium is favored by higher pressure and lower temperature. However, pressure increase leads to a trade-off between product yield and operating cost, and operation below 220 °C makes it difficult to overcome the activation energy of CO_2 conversion given its stability, requiring development of better catalysts [44]. In this sense, Figure 6 shows the effect of varying operating conditions on the reaction performance of CO_2 hydrogenation to methanol, where lower temperatures are unveiled to also benefit methanol selectivity. Alternatively to conventional gas-phase synthesis, other technologies have been developed. An example is to perform in situ distillation to improve the yield by water removal [42] and to employ supersonic separators in the synthesis loop [45].

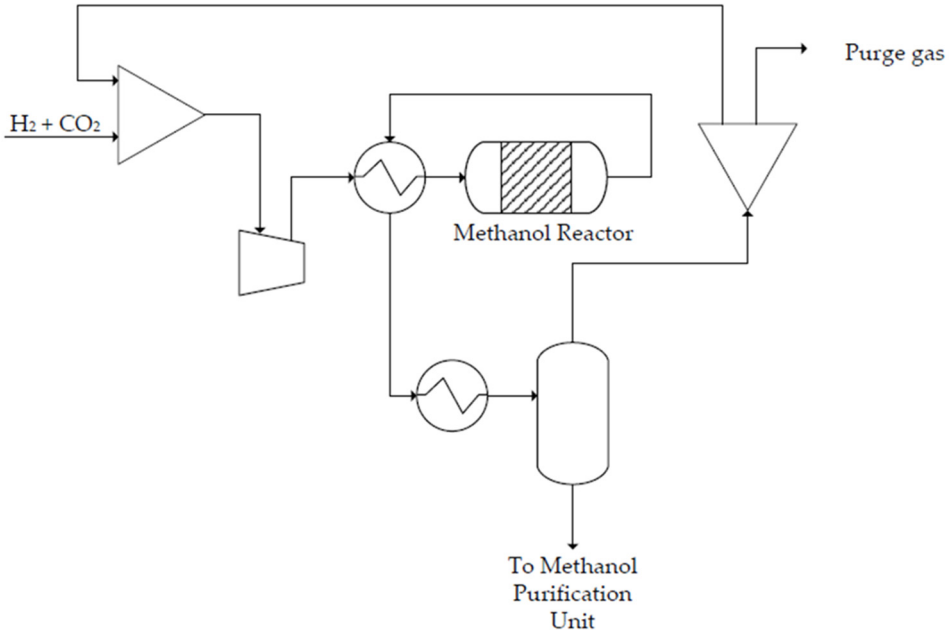

Figure 5. Synthesis loop of CO_2 hydrogenation to methanol.

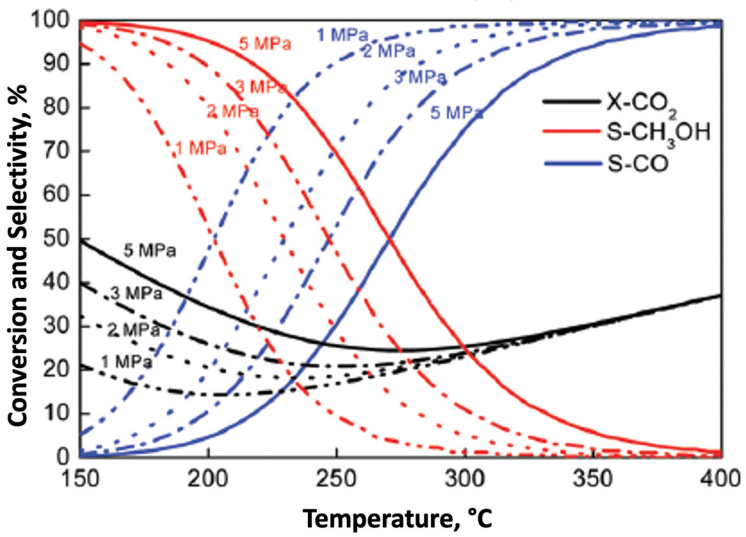

Figure 6. Chemical equilibrium of CO_2 hydrogenation to methanol at different temperatures and pressures (stoichiometric feed H_2:CO_2 3:1): CO_2 conversion, selectivity to methanol, and selectivity to CO. Reprinted with permission from [46].

CO_2 hydrogenation to methanol has been carried out through different methods, including heterogeneous and homogeneous catalysis, in addition to less common approaches like photocatalysis, electrocatalysis, and enzymatic catalysis [47]. All these catalytic methods are well described and compared in a recent review work [47]. CO_2 hydrogenation catalysts usually contain copper or a noble metal as the active species, often being a bimetallic and/or a hybrid oxide catalyst. Copper catalysts for this application are usually associated to ZnO with Al_2O_3 as a supporter, which improves the dispersion of active sites over the surface. Also, ZrO_2 addition offers greater mechanical and thermal stability, and it is often coupled to copper for CO_2 hydrogenation to methanol. Its hydrophilicity and large specific surface area improve its performance compared to the conventional catalyst formulation utilized for syngas conversion ($Cu/ZnO/Al_2O_3$). Research has shown that it is possible to achieve good methanol selectivity by using Ga_2O_3, La_2O_3, Y_2O_3, and MgO promoters [39]. Promoters play a crucial role as one of the major components, alongside the active metal

and the support. While the promoter itself may not participate in the desired reaction, it significantly influences the catalyst's active components. This influence can manifest in facilitating the reaction or reducing the production of unwanted byproducts. Consequently, the use of promoters enhances both the catalyst's activity and the selectivity of the resulting product. There are two main types of promoters: structural and electronic. Structural promoters, considered inert, stabilize the catalyst under conditions that prevent sintering of active catalyst particles. On the other hand, electronic influencers increase the electronic density of the catalyst's active portion, by either increasing or decreasing the number of active metals [48,49]. Recent review works from Din et al. [48] and Azhari, N. J. et al. [49] cover this topic. Several types of catalysts and promoters and their behavior from the mechanism point of view are reviewed in both works. The authors provide an in-depth discussion about the influence of the promoters on this catalytic process.

The water generated by CO_2 hydrogenation (Equation (6)) may lead to sintering and rapid agglomeration of a copper catalyst, thus reducing its activity. In contrast, noble metals (e.g., Pd, Au) are more stable and resistant to sintering, while being alternatives to copper and capable of ensuring good catalytic performance. These catalysts also involve the use of promoters: palladium uses ZnO, Ga_2O_3, CeO_2, and/or SiC, while gold catalysts use ZnO, TiO_2, ZrO_2, TiC, and/or CeOx. The use of ZnO allows much higher selectivity for methanol.

The preparation of the catalyst is important to ensure large surface density and good distribution of the active sites, for the best reaction performance. Several preparation methods have been considered on a lab scale, with the classical method being co-precipitation of components with hydroxides (or carbonates) or another precipitating agent, which is followed by washing, filtration, drying, calcination, and grinding [50]. A further technique largely adopted in the literature is impregnation. In addition to the catalysts mentioned above, other types have shown good catalytic activity for CO_2 hydrogenation. These are mostly oxides (e.g., In_2O_3/ZrO_2, MnOx/m- Co_3O_4, ZnO- ZrO_2) [46]. Table 2 gives a summary of the type of catalysts, their preparation method, synthesis conditions, and performance.

Table 2. Catalysts for CO_2 hydrogenation to methanol: methods of preparation, synthesis conditions, and their yields. Adapted with permission from [46,47].

Catalyst	Preparation	Temperature (°C)	Conversion (%)	Selectivity (%)
$Cu/ZnO/Al_2O_3$ [51]	Physical mixture	270	10.9	72.7
$Cu/Zn/Ga/SiO_2$ [52]	Co-impregnation	270	5.6	99.5
Cu/Ga/ZnO [53]	Co-impregnation	270	6.0	88.0
CuZnGa-LDH [54]	AMOST *	270	≈20	≈49
$Cu@ZnO_x$ [55]	Precipitation	250	2.3	100
Cu/Zn/Al/Y [56]	Co-precipitation	250	26.9	52.4
$Cu/ZnO/ZrO_2$ [57]	Inverse co-precipitation	240	17.5	48.4
$Cu/Zn/ZrO_2$ [58]	Combustion Glycerine-Nitrate	220	12.0	71.1
$Cu/Zn/ZrO_2$ [59]	Combustion Urea-Nitrate	220	5.8	72
Cu/Ga_2O_3/NC ZrO_2 [60]	Deposition-precipitation	250	13.7	75.6
$Cu/ZnO/ZrO_2/Ga_2O_3$ [61]	Co-precipitation	250	-	75
$Cu/ZnO/ZrO_2/Ga_2O_3$ [61]	Complexation with citrate	220	-	70
Ga-Cu-ZnO- ZrO_2 [62]	Co-precipitation	250	22	72
Cu-ZnO-ZrO_2 [63]	Inverse co-precipitation	240	9.7	62
Cu-ZnO-ZrO_2 [64]	Co-precipitation with oxalate	240	9	-
Cu-ZnO-ZrO_2 [65]	Co-precipitation with surfactants	240	12.1	54.1
Cu/ZrO_2 [66]	Deposition-precipitation	240	6.3	48.8
$La_{0.8}$ $Zr_{0.2}$ $Cu_{0.7}$ $Zn_{0.3}$ O_x [67]	Sol-gel	250	12.6	52.5
CuZn@UiO-bpy [68]	In situ reduction	250	3.3	100
Pd/Al_2O_3/ZSM-5 [69]	Co-precipitation	260	16.9	2.1
$Pd/ZnO/Al_2O_3$ [70]	Deposition-precipitation	180	29	79.4
PdZn-400 [71]	Pyrolysis Pd@ZIF-8	270	15.1	56.2
Pd/on Ga_2O_3 [72]	Impregnation	250	17.3	51.6

Table 2. *Cont.*

Catalyst	Preparation	Temperature (°C)	Conversion (%)	Selectivity (%)
Pd/Zn/CNTs [73]	Impregnation	250	6.3	99.6
Pd/In_2O_3 [74]	Impregnation	300	20	70
Au/ZnO [75]	Deposition-precipitation	240	0.3	82
Pd-Cu/SBA-15 [76]	Impregnation	250	6.5	23
$Pd-Cu/SiO_2$ [76]	Impregnation	250	6.6	34
PdZnAl [77]	Co-precipitation	250	0.6	60
NiGa SiO_2 [78]	Impregnation	200	-	-
$Cu_{11}In_9$—In_2O_3 [79]	Co-precipitation	280	11.4	80.5
In_2O_3/ZrO_2 [80]	Impregnation	300	5.2	99.8
ZnO/ZrO_2 [81]	Co-precipitation	320	10	91
Ga_2/ZrO_x [82]	Co-precipitation	300	12.4	80
$Cu-ZnO/Al_2O_3$ [83]	Co-precipitation	260	65.8	77.3
Pd/ZnO [84]	Sol-immobilization	250	10.7	60
h-In_2O_3-R [85]	Precipitation	300	6.7	99.5
CuZn [86]	Pseudo Sol-Gel	280	14.0	53
FL-MoS_2 [87]	-	180	12.5	94.3
$Co@Si_{0.95}$ [88]	Co-precipitation	320	11	54

* AMOST = Aqueous miscible organic solvent treatment.

Good catalytic performances have also been observed in homogeneous catalysis, in particular with the use of noble metals (e.g., based on Ru and Ir), but the high cost of these components has aroused research on Co-, Fe-, and Mn-based homogeneous catalysts that are active at temperatures as low as 100 °C. Complexes of metals and phosphines form the pre-catalysts, with an example being [Ru(tdppcy)($C(CH_2)_3$)] [47]. The reaction then takes place at nearly ambient temperature and at high pressure (≈60 bar).

5. Methanol to Formaldehyde Oxidation Unit

Currently, the industrial production of formaldehyde occurs via catalytic partial oxidation of methanol. However, the first production of formaldehyde from methanol was made with a high temperature process (600 °C) using a silver catalyst without oxygen supply following the following Reaction (9):

$$CH_3OH \rightarrow CH_2O + H_2 \quad (9)$$

Since the process is highly exothermic, temperature control is key to ensure good selectivity, so the reactors are typically designed with circulation of saturated water for generation of high-pressure steam, usually with the reaction occurring within tubes filled by the catalyst [89]. The catalyst choice is crucial because other reactions in parallel and in sequence can occur, reducing selectivity to formaldehyde formation. The overall desired reaction is presented in Equation (10), and two other secondary reactions are shown in Equations (11) and (12) [90]. Research has been carried out to develop a stable catalyst capable of producing formaldehyde with relatively high yields at lower temperatures [90].

$$CH_3OH + 0.5O_2 \rightarrow CH_2O + H_2O \quad (10)$$

$$CH_3OH + 0.5O_2 \rightarrow CH_2O + H_2O \quad (11)$$

$$CH_2O + O_2 \rightarrow CO_2 + H_2O \quad (12)$$

Currently, three industrial processes are commercially available for producing formaldehyde from methanol: BASF, ICI-silver, and FORMOX [91]. Both BASF and ICI employ a fixed bed of silver-based catalysts, which operates at atmospheric pressure with a large excess of methanol. The operating temperature is higher in the BASF process (650–720 °C) [92], where methanol conversion can reach 98%. The ICI-silver process operates at 600–650 °C and has a lower methanol conversion of 77–87%, requiring recycling of

unconverted reactant (recovered by distillation). The yields are 86.5–90.5% and 87–92% for the BASF and the ICI-silver processes, respectively.

The problem of high reaction temperature required by silver catalysts makes it more difficult to control the advance of oxidation reactions and also minimizes bed lifetime (i.e., due to catalyst sintering and aggregation) [93]. To overcome these issues and improve plant performance, an iron-molybdenum catalyst active at 250–400 °C was developed [49], being capable of reaching a yield of 88–92% [91] with a methanol conversion of 98–99%. It substantially outperforms older high-temperature silver catalysts, whose yield is around 86%. The catalyst is the main working basis of the FORMOX reactor, which comprises a fixed bed operated with methanol excess at 250–400 °C and at atmospheric pressure. The product gas is cooled and sent to water-scrubbing to separate formaldehyde from the gaseous phase. The bottom product is aqueous formaldehyde 37–55%w with <1%w methanol [94]. A typical flowsheet of this process is given in Figure 7. The FORMOX process has become the new standard for formaldehyde production and is already widely used in the industry. As a partial oxidation process, the oxygen/methanol ratio is a key parameter to ensure the control of oxidation reactions. The oxygen content in the reactant mixture should not be too high—to avoid losing product selectivity and prevent excess heat generation by oxidation reactions—nor too low—to avoid catalyst deactivation. In this sense, Figure 8 illustrates the recommended window of operating conditions for oxygen and methanol contents in the reactor inlet [95].

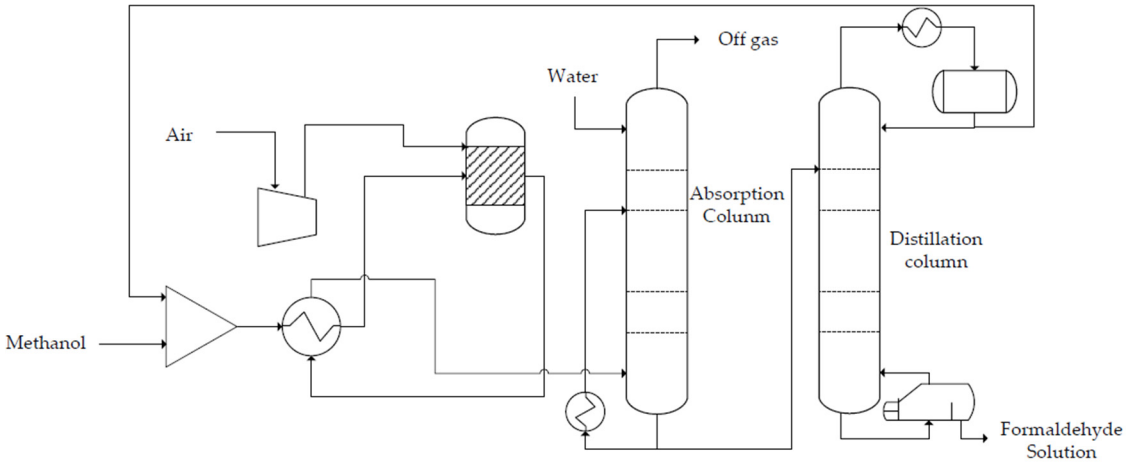

Figure 7. Production of aqueous formaldehyde (35–55%w) from methanol partial oxidation via the FORMOX process. Adapted from [94].

Beyond iron molybdate and silver, other active species have been tested. For instance, good catalytic activity was also unveiled with the use of alloys $Zr(MoO_4)_3$ and $Ce_2(MoO_4)_3$. Performance comparison with the standard FORMOX formulation is shown in Figure 9a, where formaldehyde yield is presented as a function of methanol conversion [96]. Similarly, interesting catalytic properties in using vanadium associated to different elements were also shown in the literature, as shown in Figure 9b [96], where $FeVO_4$ and $AlVO_4$ catalysts were evidenced as capable of reaching 76–87% of selectivity to formaldehyde when methanol conversion is above 50% (on the other hand, other metal catalysts associated with vanadium show a more or less low catalytic activity for oxidation).

The preparation of the catalyst and the quantity required is linked to operating conditions, design type, and specificities of the reactor used in the process, thus affecting capital investment and catalyst reposition costs. Improper preparation method and unnecessarily large amounts encumber the process and may entail long-term losses by active surface reduction as a result of abrasion, fragmentation, and deactivation. The preparation method is critical for yielding a material with good resistance to mechanical stresses. The most widely used preparation method of catalysts for industrial scale applications is co-precipitation.

A common procedure of this type to prepare formaldehyde catalysts of iron molybdate is to mix ammonium heptamolybdate with an aqueous solution of $FeCl_3$. The mixture forms a precipitate, which is filtered and calcined after washing at 400–450 °C. The product comprises MoO_3 crystals (surface area 5–8 m^2/g) and an $Fe_2(MoO_4)_3$ catalyst, which is applicable to formaldehyde production.

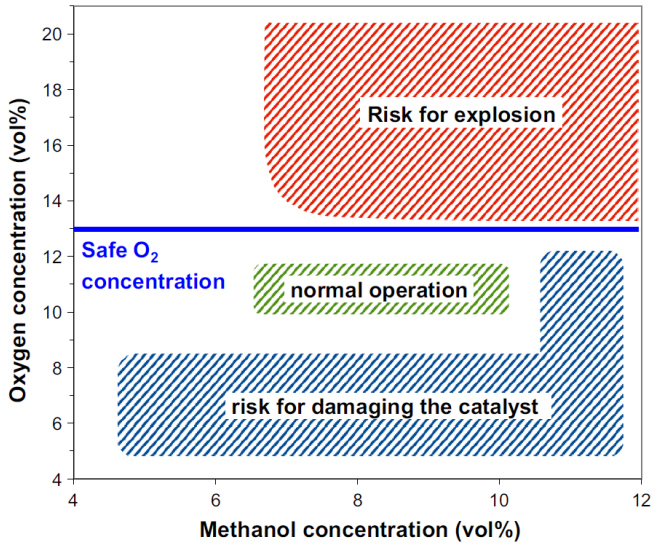

Figure 8. Operating conditions of methanol partial oxidation via the FORMOX process: O_2 and methanol content in the reactor inlet. Reprinted with permission from ref. [96].

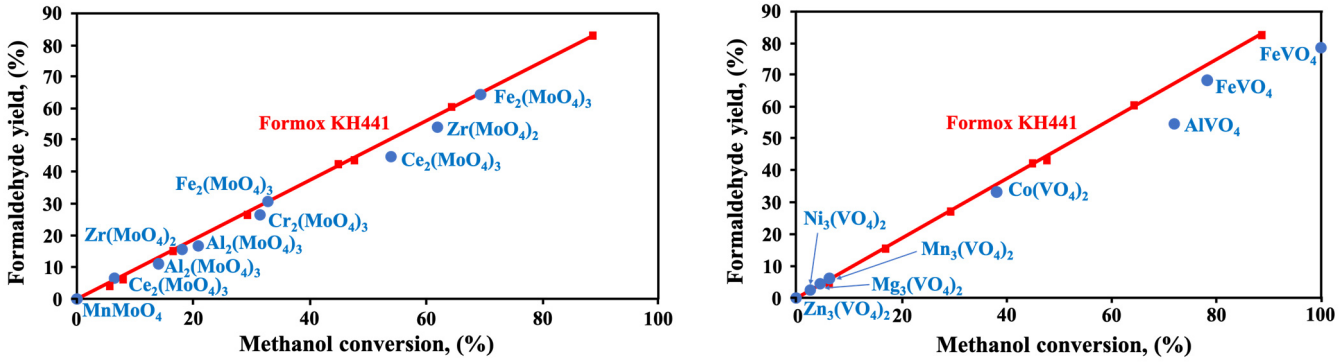

(**a**) (**b**)

Figure 9. Comparison between commercial Formox KH44L and alternative catalysts for formaldehyde production (feed conditions: 300 °C, 6%v methanol): (**a**) molybdate-based and (**b**) vanadate-based catalysts. Adapted with permission from [96].

Some drawbacks of the co-precipitation method are the relatively high cost of reagents, high water consumption, the considerable release of gas in the form of impurities, and the relatively small surface area, which results in a shallow rate of reoxidation of the spent catalyst [97]. Thus, research has been carried out to overcome the limitations of co-precipitation. For instance, the sol-gel approach has been proposed [98], offering the advantage of low temperature preparation, which avoids the volatilization of molybdate, ensuring good distribution/dispersion of MoO_3 on $Fe_2(MoO_4)_3$. While it is capable of reasonable selectivities, the activity is much lower than that of the co-precipitation catalyst, and its mechanical strength is also inferior.

In addition to these methods, research on catalyst preparation by hydrothermal methods has emerged [99]. The iron solution and molybdate are thermally treated at 150 °C in an autoclave reactor. The catalyst is obtained without calcination after washing, filtering,

and drying. However, the resulting catalyst shows instability at higher temperatures (from 250–300 °C), and its surface can be easily changed. Alternatively, the mechanochemical preparation of iron molybdate catalysts has been developed [100]. The method is much simpler to implement compared to co-precipitation. Indeed, it does not use any solvents. The preparation is performed in a mill, giving the outlet a circular catalyst and allowing it to reach a selectivity of 97.56%. However, the crystals are not uniform, and the grinding time is much longer (about 2 h).

Recently, a mixing/evaporation technique was developed [97] to prepare the catalyst. Ammonium molybdate is dissolved in water before the addition of iron nitrate powder (dropwise). The catalyst is obtained after evaporation, drying, and calcination. In order to reduce the preparation temperature, other methods were developed, such as grinding and centrifugation of molybdic acid and iron oxalate [101]. Given what is presented, it can be deduced that a large number of physicochemical preparation methods have been developed for the iron molybdite catalyst. Each technique has its advantages and disadvantages, but co-precipitation remains dominant in industrial applications. Determining the iron/molybdate ratio is vital in defining the active phase of the catalyst. For this purpose, Söderhjelm and colleagues dispersed Mo on $Fe_2(MoO_4)_3$ and estimated that the catalyst has an active phase when the Mo/Fe ratio = 1.7 [95]. The authors showed that the Mo/Fe ratio strongly affect the conversion of the methanol. The highest conversion was observed for the lowest Mo/Fe ratio (55% for the 0.2 ratio). The Mo/Fe ratio permitted also to obtain highest specific surface area (55.4 m^2/g for 0.2 ratio). However, as expected highest conversion does not permit to obtain high selectivity to formaldehyde. In this case the best results was observed at low conversion (90% selectivity for the Mo/Fe ratio of 2.2 at 256 °C) [95].

6. Formaldehyde Carbonylation to Glycolic Acid

The flowsheet of a carbonylation process for glycolic acid production is shown in Figure 10 [32] In the reactor, formaldehyde undergoes carbonylation in the presence of an acid catalyst to produce the glycolic acid. The most relevant reactions in this regard are shown in Equations (13)–(15), which represent the desired synthesis of glycolic acid, the overall secondary reaction of dimer formation from formaldehyde and CO, and the dimerization of glycolic acid (another secondary reaction). Aqueous formaldehyde solution is fed to the synthesis loop together with carbon monoxide, and the mixture is preheated to the reactor inlet temperature before entering the reactor. The reaction products are then separated in a flash, where the raw product is recovered. A major part of unreacted tail-gas from the synthesis loop high-pressure drum is recirculated in the process. The condensed liquid (glycolic acid concentrated liquid) is fed to a distillation column to separate the water from reaction products. The glycolic acid solution has a mass fraction of approximately 81%. This solution is then fed into a crystallizer, forming a liquid–solid mixture. Finally, a centrifugal filter collects the solid glycolic acid after solid–liquid separation [32].

$$CH_2O + H_2O + CO \rightarrow HOCH_2COOH \quad (13)$$

$$2CH_2O + H_2O + 2CO \rightarrow HOCH_2COOCH_2COOH \quad (14)$$

$$2HOCH_2COOH \rightarrow HOCH_2COOCH_2COOH + H_2O \quad (15)$$

The control of the operating conditions and the use of a suitable catalyst is essential to conversion of formaldehyde with good selectivity to glycolic acid. Early processes for this route used to employ sulfuric acid [102]. DuPont started commercial production of glycolic acid as an intermediary in the production of ethylene glycol. This production process operated from 1940 to 1968. In this process, the formaldehyde was produced from syngas, and the catalyst was H_2SO_4; the temperature was higher than 200 °C, and the pression higher than 60 MPa. In 1974, Chevron submitted a patent in which they proposed a process to produce glycolic acid. They were able to propose a process with a lower temperature when compared to the DuPont process, since the higher temperature reported in the patent

was 50 °C. They could reduce the pressure of the process compared to DuPont's process, but they also struggled with the high-pressure demand of the process, which varied from 6.9 MPa to 13.8 MPa [103]. Table 3 presents the main catalysts reported in the literature used to produce glycolic acid from formaldehyde.

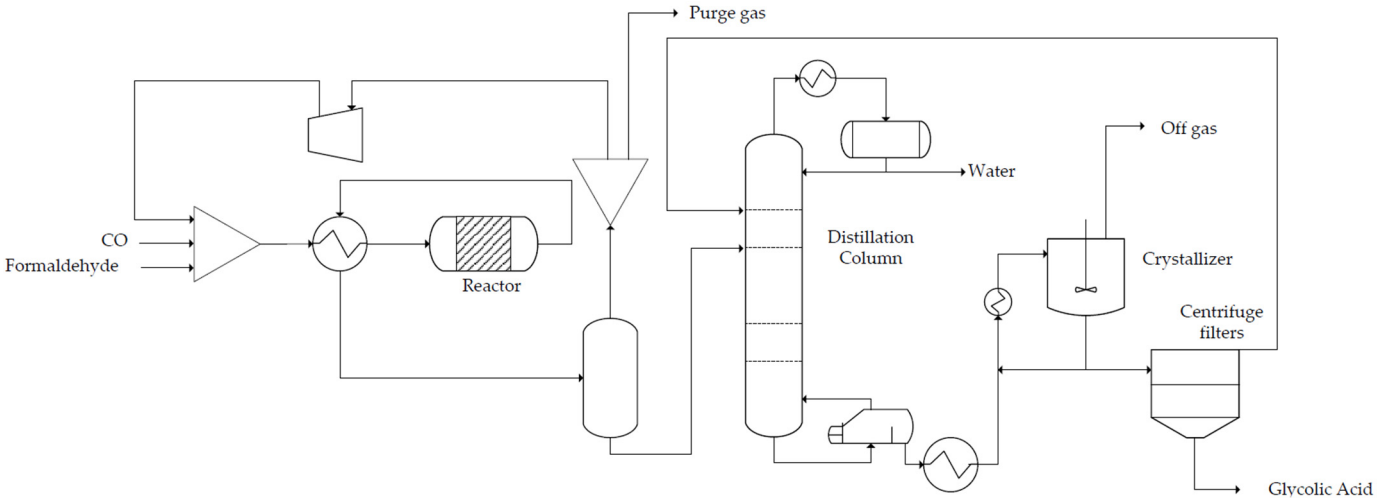

Figure 10. Process flowsheet of formaldehyde carbonylation to glycolic acid. Adapted from [32].

Table 3. Catalysts used to produce glycolic acid.

Catalyst	T	P	X	S	Y	Ref.
H_2SO_4	204–220 °C	64.1 MPa	-	-	89.3%	[104]
Nickel iodide on silica gel	200 °C	59.6 MPa	42.5%	-	-	[105]
Cobalt iodide on silica gel	215 °C	60.2 MPa	34.0%	-	-	[105]
Ferrous iodide on silica gel	230 °C	60.6 MPa	25.9%	-	-	[105]
HF	50 °C	6.9 MPa	100%	94% *	94%	[106]
30% $Cs_{2.5}H_{0.5}PW/USY$	120 °C	40 MPa	-	-	75.6%	[107]
30% $H_3PW_{12}O_{40}/USY$	120 °C	40 MPa	-	-	79.8%	[107]
$H_3PW_{12}O_{40}$	120 °C	3 MPa	-	-	82%	[108]
PDS-1.0	120 °C	6.0 MPa	99.9%	68.8% *	68.8%	[109]
PDS-1.0-F	120 °C	6.0 MPa	99.9%	91.2% *	91.2%	[109]
CF_3SO_3H	120 °C	6.0 MPa	99.8%	94.8% *	94.8%	[109]
PdO/ZSM-5	130 °C	4 MPa	50.2%	-	-	[110]
PtO/ZSM-5	130 °C	4 MPa	50.3%	-	-	[110]
Ru_2O_3/ZSM-5	130 °C	4 MPa	50.2%	-	-	[110]
Rh_2O_3/ZSM-5	130 °C	4 MPa	50.2%	-	-	[110]

* Selectivity calculated based on the conversion and yield results.

The optimal acidity of a catalyst for formaldehyde carbonylation is a delicate balance between their nature and strength. Too-strong acidity may lead to undesired side reactions or catalyst deactivation, while insufficient acidity can hinder the formation of crucial intermediates. Catalysts with tailored acidity profiles can enhance the selectivity and efficiency of glycolic acid production. Researchers in the field are actively exploring various catalyst formulations, including supported metal catalysts and mixed metal oxides, to fine-tune the acidity and achieve better control over the carbonylation process. Understanding the impact of acidity on the catalytic performance is essential for advancing the development of efficient and selective catalysts for the sustainable synthesis of glycolic acid. As can be seen from Table 3, the high yields of glycolic acid (up to 80%) were obtained using supported heteropolyacids on zeolites. High activity and yield for glycolic acid were also observed using polymer-based catalysts modified with sulfonic groups. The grafted sulfonic groups presented lower density of the acid sites but much stronger sites, yielding 95% glycolic acid compared to 68.8% obtained in the case of the non-modified sample.

Noble metal oxides such as PdO, Rh_2O_3, and Ru_2O_3 were also tested, but the conversion was much lower (50%) than for the strong acid catalysts (almost 100% in the case of PDS catalysts). Even the incorporation of ZSM-5 did not result in high yields. The nature of the acid sites is crucial. Sulfonic groups have strong Brønsted acidity, while ZSM-5 presents Brønsted–Lewis acidity. In the case of supported metal oxides on ZSM-5, one could expect the increase of the Lewis acidity, as highly dispersed PdO can be anchored on the ZSM-5 surface through the interaction between PdO and Brønsted acid sites. This could explain the low activity of these materials.

7. Conclusions

In this work, indirect production of glycolic acid from H_2 and CO_2 was discussed regarding existing technological alternatives, their operating conditions, and the characteristics of the involved catalysts in the overall process, which comprises the following sections: CO_2 capture, H_2 production from water electrolysis, CO_2 hydrogenation to methanol, selective methanol oxidation, and formaldehyde carbonylation to glycolic acid. All steps are presented in a combined flowsheet in Figure 11.

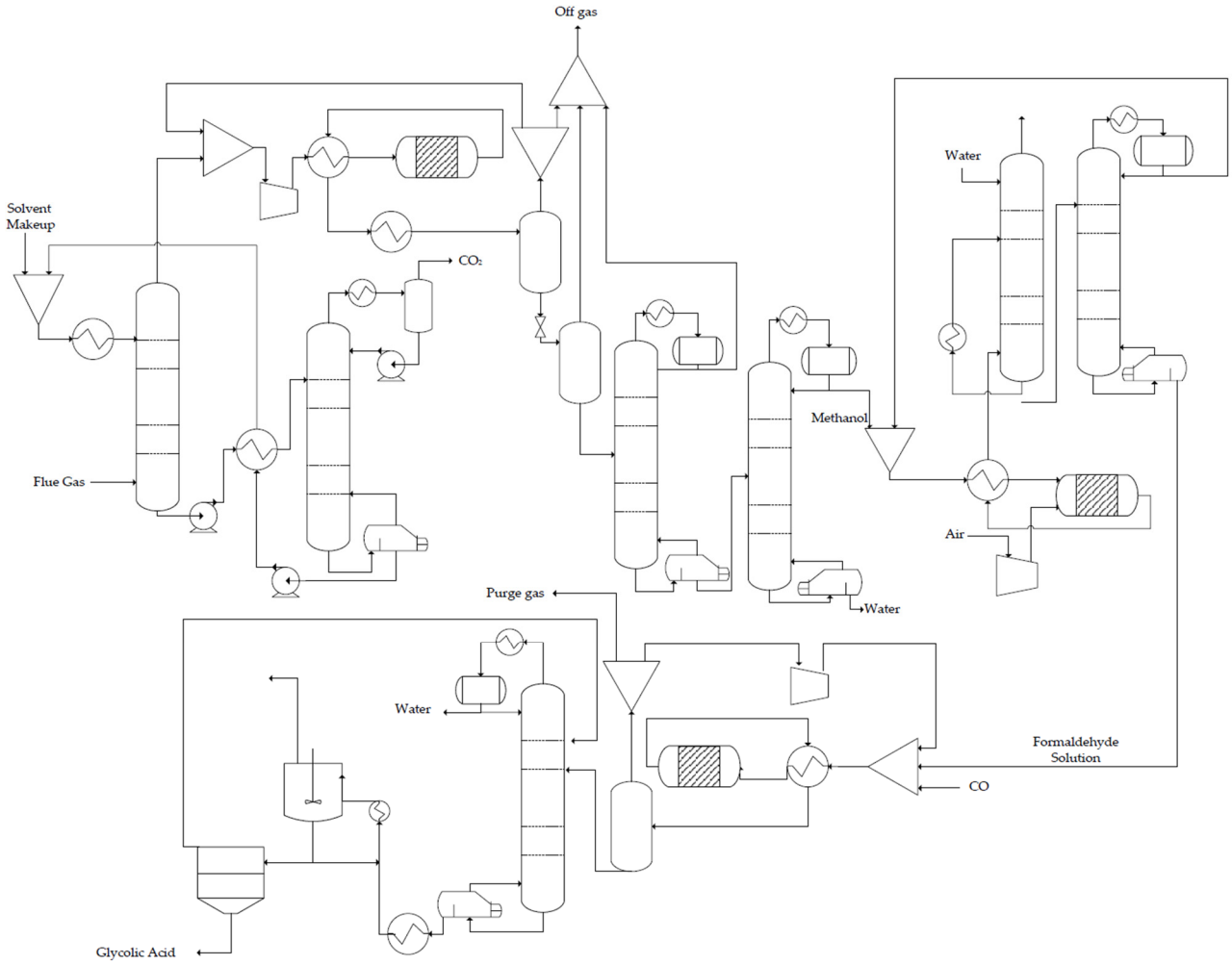

Figure 11. Process flowsheet of CO_2 to glycolic acid.

The choice of the method for CO_2 capture depends on the characteristics of the fuel and exhaust gas from combustion, where abatement costs are expected to increase with reduced carbon content and lower gas pressure. Post-combustion chemical absorption is usually better for CO_2 at low partial pressure, pre-combustion allows in situ generation of H_2—eventually dismissing electrolysis and even the capture of CO_2 from syngas,

thus being advantageous to couple methanol production to power generation—and oxy-combustion is best suited to high carbon contents (e.g., biomass as energy resource), dispensing CO_2 separation in exchange for oxygen production. Regarding water electrolysis, proton exchange membrane technology using noble metals in the electrodes appears as the most promising for deployment within a short- to medium-term horizon—given the relatively high energy efficiency and TRL of 6–7—being capable of producing pure green hydrogen (up to 99.99%v) from wind and solar energy. CO_2 hydrogenation to methanol adopts a similar process of conventional plants on the synthesis loop and product purification, demanding small changes in the reactor catalyst—due to low carbon monoxide and greater H_2O content—to enhance product yield.

The catalyst of CO_2 hydrogenation can be of a similar type to that of conventional methanol synthesis, which is usually essentially $Cu/ZnO/Al_2O_3$ prepared by co-precipitation with the addition of promoters; zirconia addition has been shown to be particularly advantageous for this application. The selective oxidation to formaldehyde is carried out preferentially through the FORMOX route over iron molybdate catalysts (Mo/Fe ratio 1.7) at 250–400 °C and at atmospheric pressure, with strict control of air injection, which allows reaching high yields (88–92%). Finally, the carbonylation of formaldehyde can be approached over polymer-modified resins (PDS, Table 3), reaching almost 95% glycolic acid yield at 120 °C and 6 MPa.

Individually, an estimation of the TRL levels for the individual steps in this complex CO_2-to-glycolic acid process can be done: (i) CO_2 capture with amines is estimated to be at TRL level of 8. This is already well-established technology for CO_2 capture in various industries, including power plants; (ii) CO_2 hydrogenation to methanol is considered to be at TRL level of 7. CO_2 hydrogenation to methanol using CuZnAl-type catalysts is a technology with a relatively high TRL. Pilot-scale demonstrations contribute to its maturity; (iii) Methanol oxidation to formaldehyde has seen significant progress, but it may not be as mature as the previous steps. Research and development efforts, including catalyst improvements, have elevated its TRL to 6, but larger-scale implementations are needed for further maturity; (iv) formaldehyde carbonylation to glycolic acid is likely at a lower TRL (5) compared to the previous steps. While there are established processes for formaldehyde carbonylation, optimizing and scaling up the process for glycolic acid production may still require additional research and development. However, it is important to note that these TRL estimates are generalizations and can vary based on the specific technologies, catalysts, and processes employed in each step. Actual TRL levels may be influenced by the specific advancements achieved in ongoing research and development projects in the field of CO_2 valorization.

Future studies can contribute to advancing the state of the art in glycolic acid production from CO_2, fostering sustainability and efficiency in this important chemical synthesis process. It is important to focus on optimizing CO_2 capture techniques, considering the specific characteristics of different fuel sources and exhaust gases. Exploring advanced capture technologies and evaluating their economic feasibility under various conditions would enhance the overall efficiency of the glycolic acid production process. The hydrogenation of CO_2 requires huge quantities of hydrogen. Research efforts should delve into advancing water electrolysis technologies, particularly exploring alternative materials for electrodes and catalysts. Investigating novel electrocatalysts and materials could contribute to improving the energy efficiency and sustainability of the proton exchange membrane technology. In the field of CO_2 hydrogenation, the studies on catalyst development should focus on enhancing the performance and stability of catalysts, specifically exploring the role of promoters and alternative compositions. Investigating innovative catalyst design strategies may lead to improved yields and process efficiency. Researchers may also explore alternative pathways for methanol synthesis that diverge from conventional plants. Investigating innovative approaches to the synthesis loop and purification processes could contribute to process intensification and increased methanol production efficiency. One of the most challenging steps in this process is the selective oxidation of methanol to formalde-

hyde. This process plays a crucial role in the overall glycolic acid synthesis. Future studies could focus on developing advanced catalytic systems and exploring new catalyst formulations or modifications that enhance selectivity, yield, and operational stability. In addition, new studies on direct photocatalytic conversion of CO_2 to formaldehyde are also in progress. This could remove one step from the overall CO_2-to-glycolic acid process. Further investigations into the carbonylation of formaldehyde could aim to achieve a deeper understanding of the underlying processes. Exploring alternative catalysts, reaction conditions, and process intensification techniques may lead to improvements in glycolic acid yield and purity. The main progress could be made in the integration of this complex process. Future research could explore the integration of individual process steps to achieve a more streamlined and efficient overall glycolic acid production process. Investigating synergies between different stages and optimizing the overall process flow could lead to higher productivity and reduced energy consumption. Consideration of sustainable and renewable feedstocks, such as biomass-derived sources, could be explored to further align the glycolic acid production process with green and circular economy principles. Assessing the feasibility and environmental impact of alternative feedstocks would contribute to the sustainability of the entire process.

What is still missing in the literature is comprehensive economic and technological feasibility analyses for the entire glycolic acid production process, considering different scenarios and scales; this would provide valuable insights for industrial implementation. Evaluating the economic viability of each process step and identifying potential bottlenecks can guide further optimization efforts.

Author Contributions: Conceptualization, N.O.S. and R.W.; methodology, N.O.S.; data curation, N.O.S. and M.T.L.; writing—original draft preparation, N.O.S., M.T.L. and R.W.; writing—review and editing, M.T.L., R.W., G.V.B. and I.I.J. visualization, I.I.J., G.V.B. and R.W. supervision, R.W.; project administration, R.W. All authors have read and agreed to the published version of the manuscript.

Funding: This research received no external funding.

Data Availability Statement: No new data were created or analyzed in this study. Data sharing does not apply to this article.

Conflicts of Interest: The authors declare no conflict of interest.

References

1. Ruiz, C.P.T.; Dumeignil, F.; Capron, M. Catalytic Production of Glycolic Acid from Glycerol Oxidation: An Optimization Using Response Surface Methodology. *Catalysts* **2021**, *11*, 257. [CrossRef]
2. Ren, F.; Liu, W. Review of CO_2 Adsorption Materials and Utilization Technology. *Catalysts* **2023**, *13*, 1176. [CrossRef]
3. Lau, H.C.; Ramakrishna, S.; Zhang, K.; Radhamani, A.V. The Role of Carbon Capture and Storage in the Energy Transition. *Energy Fuels* **2021**, *35*, 7364–7386. [CrossRef]
4. Benetto, E.; Gericke, K.; Guiton, M. *Designing Sustainable Technologies, Products and Policies*; Springer: Berlin/Heidelberg, Germany, 2020. [CrossRef]
5. Rafiee, A.; Rajab Khalilpour, K.; Milani, D.; Panahi, M. Trends in CO_2 Conversion and Utilization: A Review from Process Systems Perspective. *J. Environ. Chem. Eng.* **2018**, *6*, 5771–5794. [CrossRef]
6. Meylan, F.D.; Moreau, V.; Erkman, S. CO_2 Utilization in the Perspective of Industrial Ecology, an Overview. *J. CO_2 Util.* **2015**, *12*, 101–108. [CrossRef]
7. Salvi, B.L.; Jindal, S. Recent Developments and Challenges Ahead in Carbon Capture and Sequestration Technologies. *SN Appl. Sci.* **2019**, *1*, 885. [CrossRef]
8. Raza, A.; Gholami, R.; Rezaee, R.; Rasouli, V.; Rabiei, M. Significant Aspects of Carbon Capture and Storage—A Review. *Petroleum* **2019**, *5*, 335–340. [CrossRef]
9. IEA GHG. *CCS Industry Build-Out Rates-Comparision with Industry Analogues*; Pure Offices, Cheltenham Office Park: Cheltenham, UK, 2017.
10. Haszeldine, R.S.; Flude, S.; Johnson, G.; Scott, V. Negative Emissions Technologies and Carbon Capture and Storage to Achieve the Paris Agreement Commitments. *Philos. Trans. R. Soc. A Math. Phys. Eng. Sci.* **2018**, *376*, 20160447. [CrossRef]
11. Abanades, J.C.; Rubin, E.S.; Mazzotti, M.; Herzog, H.J. On the Climate Change Mitigation Potential of CO_2 Conversion to Fuels. *Energy Environ. Sci.* **2017**, *10*, 2491–2499. [CrossRef]

12. Cuéllar-Franca, R.M.; Azapagic, A. Carbon Capture, Storage and Utilisation Technologies: A Critical Analysis and Comparison of Their Life Cycle Environmental Impacts. *J. CO_2 Util.* **2015**, *9*, 82–102. [CrossRef]
13. He, X.; Guo, X.; Xia, G.; Xu, R.; Wu, Y.; Luan, X. A Green Route to Methyl Formate from CO_2-Derived Formamides over Solid Base Catalysts. *Catalysts* **2023**, *13*, 487. [CrossRef]
14. Schuler, E.; Demetriou, M.; Shiju, N.R.; Gruter, G.J.M. Towards Sustainable Oxalic Acid from CO_2 and Biomass. *ChemSusChem* **2021**, *14*, 3636–3664. [CrossRef] [PubMed]
15. Samantaray, P.K.; Little, A.; Haddleton, D.M.; McNally, T.; Tan, B.; Sun, Z.; Huang, W.; Ji, Y.; Wan, C. Poly(Glycolic Acid) (PGA): A Versatile Building Block Expanding High Performance and Sustainable Bioplastic Applications. *Green. Chem.* **2020**, *22*, 4055–4081. [CrossRef]
16. Wang, Y.; Liu, J.; Li, C.; Xiao, Y.; Wu, S.; Zhang, B. Synthesis and Characterization of Poly(Butylene Terephthalate-Co-Glycolic Acid) Biodegradable Copolyesters. *Eur. Polym. J.* **2022**, *180*, 111613. [CrossRef]
17. Zhou, X.; Zha, M.; Cao, J.; Yan, H.; Feng, X.; Chen, D.; Yang, C. Glycolic Acid Production from Ethylene Glycol via Sustainable Biomass Energy: Integrated Conceptual Process Design and Comparative Techno-Economic-Society-Environment Analysis. *ACS Sustain. Chem. Eng.* **2021**, *9*, 10948–10962. [CrossRef]
18. Lee, C.S.; Aroua, M.K.; Wan Daud, W.A.; Cognet, P.; Pérès, Y.; Ajeel, M.A. Selective Electrochemical Conversion of Glycerol to Glycolic Acid and Lactic Acid on a Mixed Carbon-Black Activated Carbon Electrode in a Single Compartment Electrochemical Cell. *Front. Chem.* **2019**, *7*, 110. [CrossRef] [PubMed]
19. Salusjärvi, L.; Havukainen, S.; Koivistoinen, O.; Toivari, M. Biotechnological Production of Glycolic Acid and Ethylene Glycol: Current State and Perspectives. *Appl. Microbiol. Biotechnol.* **2019**, *103*, 2525–2535. [CrossRef]
20. Anwar, M.N.; Fayyaz, A.; Sohail, N.F.; Khokhar, M.F.; Baqar, M.; Khan, W.D.; Rasool, K.; Rehan, M.; Nizami, A.S. CO_2 Capture and Storage: A Way Forward for Sustainable Environment. *J. Environ. Manag.* **2018**, *226*, 131–144. [CrossRef]
21. Abotalib, M.; Zhao, F.; Clarens, A. Deployment of a Geographical Information System Life Cycle Assessment Integrated Framework for Exploring the Opportunities and Challenges of Enhanced Oil Recovery Using Industrial CO_2 Supply in the United States. *ACS Sustain. Chem. Eng.* **2016**, *4*, 4743–4751. [CrossRef]
22. Mukhtar, A.; Saqib, S.; Mellon, N.B.; Babar, M.; Rafiq, S.; Ullah, S.; Bustam, M.A.; Al-Sehemi, A.G.; Muhammad, N.; Chawla, M. CO_2 Capturing, Thermo-Kinetic Principles, Synthesis and Amine Functionalization of Covalent Organic Polymers for CO_2 Separation from Natural Gas: A Review. *J. Nat. Gas. Sci. Eng.* **2020**, *77*, 103203. [CrossRef]
23. Hatta, N.S.M.; Aroua, M.K.; Hussin, F.; Gew, L.T. A Systematic Review of Amino Acid-Based Adsorbents for CO_2 Capture. *Energies* **2022**, *15*, 7151. [CrossRef]
24. Wang, X.; Song, C. Carbon Capture From Flue Gas and the Atmosphere: A Perspective. *Front. Energy Res.* **2020**, *8*, 560849. [CrossRef]
25. Olajire, A.A. CO_2 Capture and Separation Technologies for End-of-Pipe Applications—A Review. *Energy* **2010**, *35*, 2610–2628. [CrossRef]
26. Chai, S.Y.W.; Ngu, L.H.; How, B.S. Review of Carbon Capture Absorbents for CO_2 Utilization. *Greenh. Gases Sci. Technol.* **2022**, *12*, 394–427. [CrossRef]
27. Brigagão, G.V.; de Medeiros, J.L.; Araújo, O.d.Q.F. A Novel Cryogenic Vapor-Recompression Air Separation Unit Integrated to Oxyfuel Combined-Cycle Gas-to-Wire Plant with Carbon Dioxide Enhanced Oil Recovery: Energy and Economic Assessments. *Energy Convers. Manag.* **2019**, *189*, 202–214. [CrossRef]
28. Madejski, P.; Chmiel, K.; Subramanian, N.; Kuś, T. Methods and Techniques for CO_2 Capture: Review of Potential Solutions and Applications in Modern Energy Technologies. *Energies* **2022**, *15*, 887. [CrossRef]
29. Kothandaraman, A. *Carbon Dioxide Capture by Chemical Absorption: A Solvent Comparison Study*; Massachusetts Institute of Technology: Cambridge, MA, USA, 2010.
30. Aghaie, M.; Rezaei, N.; Zendehboudi, S. A Systematic Review on CO_2 Capture with Ionic Liquids: Current Status and Future Prospects. *Renew. Sustain. Energy Rev.* **2018**, *96*, 502–525. [CrossRef]
31. Zhang, W.; Jin, X.; Tu, W.; Ma, Q.; Mao, M.; Cui, C. Development of MEA-Based CO_2phase Change Absorbent. *Appl. Energy* **2017**, *195*, 316–323. [CrossRef]
32. Wang, D.; Li, J.; Meng, W.; Wang, J.; Wang, K.; Zhou, H.; Yang, Y.; Fan, Z.; Fan, X. Integrated Process for Producing Glycolic Acid from Carbon Dioxide Capture Coupling Green Hydrogen. *Processes* **2022**, *10*, 1610. [CrossRef]
33. Ghanbari, T.; Abnisa, F.; Wan Daud, W.M.A. A Review on Production of Metal Organic Frameworks (MOF) for CO_2 Adsorption. *Sci. Total Environ.* **2020**, *707*, 135090. [CrossRef]
34. Yang, R.T. *Adsorbents: Fundamentals and Applications*; John Wiley & Sons, Inc.: Hoboken, NJ, USA, 2003.
35. Tuinier, M.J.; van Sint Annaland, M.; Kramer, G.J.; Kuipers, J.A.M. Cryogenic CO_2 Capture Using Dynamically Operated Packed Beds. *Chem. Eng. Sci.* **2010**, *65*, 114–119. [CrossRef]
36. Hossain, M.M.; de Lasa, H.I. Chemical-Looping Combustion (CLC) for Inherent CO_2 Separations—A Review. *Chem. Eng. Sci.* **2008**, *63*, 4433–4451. [CrossRef]
37. Shiva Kumar, S.; Lim, H. An overview of water electrolysis technologies for green hydrogen production. *Energy Rep.* **2022**, *8*, 13793–13813. [CrossRef]
38. Ursua, A.; Gandia, L.M.; Sanchis, P. Hydrogen Production From Water Electrolysis: Current Status and Future Trends. *Proc. IEEE* **2012**, *100*, 410–426. [CrossRef]

39. Sapountzi, F.M.; Gracia, J.M.; Weststrate, C.J.; Fredriksson, H.O.A.; Niemantsverdriet, J.W. Electrocatalysts for the Generation of Hydrogen, Oxygen and Synthesis Gas. *Prog. Energy Combust. Sci.* **2017**, *58*, 1–35. [CrossRef]
40. Brigagão, G.V.; de Queiroz Fernandes Araújo, O.; de Medeiros, J.L.; Mikulcic, H.; Duic, N. A Techno-Economic Analysis of Thermochemical Pathways for Corncob-to-Energy: Fast Pyrolysis to Bio-Oil, Gasification to Methanol and Combustion to Electricity. *Fuel Process. Technol.* **2019**, *193*, 102–113. [CrossRef]
41. Chinchen, G.C.; Denny, P.J.; Parker, D.G.; Spencer, M.S.; Whan, D.A. Mechanism of Methanol Synthesis from $CO_2/CO/H_2$ Mixtures over Copper/Zinc Oxide/Alumina Catalysts: Use Of14C-Labelled Reactants. *Appl. Catal.* **1987**, *30*, 333–338. [CrossRef]
42. Kagan, Y.B.; Rozovskii, A.Y.; Liberov, L.G.; Slivinskii, E.V.; Lin, G.I.; Loktev, S.M.; Bashkirov, A.N. Study of the Mechanism of the Synthesis of Methanol from Carbon Monoxide and Hydrogen Using the Radioactive Carbon Isotope 14C [Cu-Zn-Al_2O_3, Zn-Cr_2O_3, and Fused Fe Catalysts]. *Dokl. Chem.* **1975**, *224*, 4–6.
43. Slotboom, Y.; Bos, M.J.; Pieper, J.; Vrieswijk, V.; Likozar, B.; Kersten, S.R.A.; Brilman, D.W.F. Critical Assessment of Steady-State Kinetic Models for the Synthesis of Methanol over an Industrial $Cu/ZnO/Al_2O_3$ Catalyst. *Chem. Eng. J.* **2020**, *389*, 124181. [CrossRef]
44. Gaikwad, R.; Reymond, H.; Phongprueksathat, N.; Rudolf Von Rohr, P.; Urakawa, A. From CO or CO_2?: Space-Resolved Insights into High-Pressure CO_2 Hydrogenation to Methanol over $Cu/ZnO/Al_2O_3$. *Catal. Sci. Technol.* **2020**, *10*, 2763–2768. [CrossRef]
45. Arinelli, L.d.O.; Brigagão, G.V.; Wiesberg, I.L.; Teixeira, A.M.; de Medeiros, J.L.; Araújo, O.d.Q.F. Carbon-Dioxide-to-Methanol Intensification with Supersonic Separators: Extra-Carbonated Natural Gas Purification via Carbon Capture and Utilization. *Renew. Sustain. Energy Rev.* **2022**, *161*, 112424. [CrossRef]
46. Zhong, J.; Yang, X.; Wu, Z.; Liang, B.; Huang, Y.; Zhanga, T. State of the Art and Perspectives in Heterogeneous Catalysis of CO_2 Hydrogenation to methanol. *Chem. Soc. Rev.* **2020**, *49*, 1385–1413. [CrossRef] [PubMed]
47. Navarro-Jaén, S.; Virginie, M.; Bonin, J.; Robert, M.; Wojcieszak, R.; Khodakov, A.Y. Highlights and Challenges in the Selective Reduction of Carbon Dioxide to Methanol. *Nat. Rev. Chem.* **2021**, *5*, 564–579. [CrossRef] [PubMed]
48. Din, I.U.; Shaharun, M.S.; Alotaibi, M.A.; Alharthi, A.I.; Naeem, A. Recent Developments on Heterogeneous Catalytic CO_2 Reduction to Methanol. *J. CO2 Util.* **2019**, *34*, 20–33. [CrossRef]
49. Azhari, N.J.; Erika, D.; Mardiana, S.; Ilmi, T.; Gunawan, M.L.; Makertihartha, I.G.B.N.; Kadja, G.T.M. Methanol Synthesis from CO_2: A Mechanistic Overview. *Results Eng.* **2022**, *16*, 100711. [CrossRef]
50. AN, X.; ZUO, Y.; ZHANG, Q.; WANG, J. Methanol Synthesis from CO_2 Hydrogenation with a Cu/Zn/Al/Zr Fibrous Catalyst. *Chin. J. Chem. Eng.* **2009**, *17*, 88–94. [CrossRef]
51. Liao, F.; Huang, Y.; Ge, J.; Zheng, W.; Tedsree, K.; Collier, P.; Hong, X.; Tsang, S.C. Morphology-Dependent Interactions of ZnO with Cu Nanoparticles at the Materials' Interface in Selective Hydrogenation of CO_2 to CH_3 OH. *Angew. Chem. Int. Ed.* **2011**, *50*, 2162–2165. [CrossRef]
52. Toyir, J.; de la Piscina, P.R.; Llorca, J.; Fierro, J.-L.G.; Homs, N. Methanol Synthesis from CO_2 and H_2 over Gallium Promoted Copper-Based Supported Catalysts. Effect of Hydrocarbon Impurities in the CO_2/H_2 Source. *Phys. Chem. Chem. Phys.* **2001**, *3*, 4837–4842. [CrossRef]
53. Toyir, J.; Ramírez de la Piscina, P.; Fierro, J.L.G.; Homs, N. Catalytic Performance for CO_2 Conversion to Methanol of Gallium-Promoted Copper-Based Catalysts: Influence of Metallic Precursors. *Appl. Catal. B* **2001**, *34*, 255–266. [CrossRef]
54. Gao, P.; Zhang, L.; Li, S.; Zhou, Z.; Sun, Y. Novel Heterogeneous Catalysts for CO_2 Hydrogenation to Liquid Fuels. *ACS Cent. Sci.* **2020**, *6*, 1657–1670. [CrossRef]
55. Le Valant, A.; Comminges, C.; Tisseraud, C.; Canaff, C.; Pinard, L.; Pouilloux, Y. The Cu–ZnO Synergy in Methanol Synthesis from CO_2, Part 1: Origin of Active Site Explained by Experimental Studies and a Sphere Contact Quantification Model on Cu+ ZnO Mechanical Mixtures. *J. Catal.* **2015**, *324*, 41–49. [CrossRef]
56. Gao, P.; Li, F.; Zhao, N.; Xiao, F.; Wei, W.; Zhong, L.; Sun, Y. Influence of Modifier (Mn, La, Ce, Zr and Y) on the Performance of Cu/Zn/Al Catalysts via Hydrotalcite-like Precursors for CO_2 Hydrogenation to Methanol. *Appl. Catal. A Gen.* **2013**, *468*, 442–452. [CrossRef]
57. Arena, F.; Italiano, G.; Barbera, K.; Bonura, G.; Spadaro, L.; Frusteri, F. Basic Evidences for Methanol-Synthesis Catalyst Design. *Catal. Today* **2009**, *143*, 80–85. [CrossRef]
58. Guo, X.; Mao, D.; Lu, G.; Wang, S.; Wu, G. CO_2 Hydrogenation to Methanol over $Cu/ZnO/ZrO_2$ Catalysts Prepared via a Route of Solid-State Reaction. *Catal. Commun.* **2011**, *12*, 1095–1098. [CrossRef]
59. Guo, X.; Mao, D.; Wang, S.; Wu, G.; Lu, G. Combustion Synthesis of CuO–ZnO–ZrO2 Catalysts for the Hydrogenation of Carbon Dioxide to Methanol. *Catal. Commun.* **2009**, *10*, 1661–1664. [CrossRef]
60. Liu, X.-M.; Lu, G.Q.; Yan, Z.-F. Nanocrystalline Zirconia as Catalyst Support in Methanol Synthesis. *Appl. Catal. A Gen.* **2005**, *279*, 241–245. [CrossRef]
61. Sloczynski, J.; Grabowski, R.; Olszewski, P.; Kozlowska, A.; Stoch, J.; Lachowska, M.; Skrzypek, J. Effect of Metal Oxide Additives on the Activity and Stability of $Cu/ZnO/ZrO_2$ Catalysts in the Synthesis of Methanol from CO_2 and H_2. *Appl. Catal. A Gen.* **2006**, *310*, 127–137. [CrossRef]
62. Ladera, R.; Pérez-Alonso, F.J.; González-Carballo, J.M.; Ojeda, M.; Rojas, S.; Fierro, J.L.G. Catalytic Valorization of CO_2 via Methanol Synthesis with Ga-Promoted Cu–ZnO–ZrO_2 Catalysts. *Appl. Catal. B* **2013**, *142–143*, 241–248. [CrossRef]
63. Arena, F.; Mezzatesta, G.; Zafarana, G.; Trunfio, G.; Frusteri, F.; Spadaro, L. How Oxide Carriers Control the Catalytic Functionality of the Cu–ZnO System in the Hydrogenation of CO_2 to Methanol. *Catal. Today* **2013**, *210*, 39–46. [CrossRef]

64. Bonura, G.; Cordaro, M.; Cannilla, C.; Arena, F.; Frusteri, F. The Changing Nature of the Active Site of Cu-Zn-Zr Catalysts for the CO_2 Hydrogenation Reaction to Methanol. *Appl. Catal. B* **2014**, *152–153*, 152–161. [CrossRef]
65. Li, L.; Mao, D.; Yu, J.; Guo, X. Highly Selective Hydrogenation of CO_2 to Methanol over CuO–ZnO–ZrO_2 Catalysts Prepared by a Surfactant-Assisted Co-Precipitation Method. *J. Power Sources* **2015**, *279*, 394–404. [CrossRef]
66. Liu, J.; Shi, J.; He, D.; Zhang, Q.; Wu, X.; Liang, Y.; Zhu, Q. Surface Active Structure of Ultra-Fine Cu/ZrO2 Catalysts Used for the CO_2+H_2 to Methanol Reaction. *Appl. Catal. A Gen.* **2001**, *218*, 113–119. [CrossRef]
67. Zhan, H.; Li, F.; Gao, P.; Zhao, N.; Xiao, F.; Wei, W.; Zhong, L.; Sun, Y. Methanol Synthesis from CO_2 Hydrogenation over La–M–Cu–Zn–O (M=Y, Ce, Mg, Zr) Catalysts Derived from Perovskite-Type Precursors. *J. Power Sources* **2014**, *251*, 113–121. [CrossRef]
68. An, B.; Zhang, J.; Cheng, K.; Ji, P.; Wang, C.; Lin, W. Confinement of Ultrasmall Cu/ZnO_x Nanoparticles in Metal–Organic Frameworks for Selective Methanol Synthesis from Catalytic Hydrogenation of CO_2. *J. Am. Chem. Soc.* **2017**, *139*, 3834–3840. [CrossRef] [PubMed]
69. Navarro-Jaén, S.; Virginie, M.; Morin, J.-C.; Thuriot, J.; Wojcieszak, R.; Khodakov, A. Hybrid monometallic and bimetallic copper-palladium zeolite catalysts for direct synthesis of dimethyl ether from CO_2. *J. Mater. Sci.* **2022**, *46*, 3889–3900. [CrossRef]
70. Xu, J.; Su, X.; Liu, X.; Pan, X.; Pei, G.; Huang, Y.; Wang, X.; Zhang, T.; Geng, H. Methanol Synthesis from CO_2 and H_2 over Pd/ZnO/Al_2O_3: Catalyst Structure Dependence of Methanol Selectivity. *Appl. Catal. A Gen.* **2016**, *514*, 51–59. [CrossRef]
71. Yin, Y.; Hu, B.; Li, X.; Zhou, X.; Hong, X.; Liu, G. Pd@zeolitic Imidazolate Framework-8 Derived PdZn Alloy Catalysts for Efficient Hydrogenation of CO_2 to Methanol. *Appl. Catal. B* **2018**, *234*, 143–152. [CrossRef]
72. Zhou, X.; Qu, J.; Xu, F.; Hu, J.; Foord, J.S.; Zeng, Z.; Hong, X.; Edman Tsang, S.C. Shape Selective Plate-Form Ga_2O_3 with Strong Metal–Support Interaction to Overlying Pd for Hydrogenation of CO_2 to CH_3OH. *Chem. Commun.* **2013**, *49*, 1747. [CrossRef]
73. Liang, X.-L.; Dong, X.; Lin, G.-D.; Zhang, H.-B. Carbon Nanotube-Supported Pd–ZnO Catalyst for Hydrogenation of CO_2 to Methanol. *Appl. Catal. B* **2009**, *88*, 315–322. [CrossRef]
74. Rui, N.; Wang, Z.; Sun, K.; Ye, J.; Ge, Q.; Liu, C. CO_2 Hydrogenation to Methanol over Pd/In_2O_3: Effects of Pd and Oxygen Vacancy. *Appl. Catal. B* **2017**, *218*, 488–497. [CrossRef]
75. Hartadi, Y.; Widmann, D.; Behm, R.J. CO_2 Hydrogenation to Methanol on Supported Au Catalysts under Moderate Reaction Conditions: Support and Particle Size Effects. *ChemSusChem* **2015**, *8*, 456–465. [CrossRef] [PubMed]
76. Jiang, X.; Koizumi, N.; Guo, X.; Song, C. Bimetallic Pd–Cu Catalysts for Selective CO_2 Hydrogenation to Methanol. *Appl. Catal. B* **2015**, *170–171*, 173–185. [CrossRef]
77. Ota, A.; Kunkes, E.L.; Kasatkin, I.; Groppo, E.; Ferri, D.; Poceiro, B.; Navarro Yerga, R.M.; Behrens, M. Comparative Study of Hydrotalcite-Derived Supported Pd_2Ga and PdZn Intermetallic Nanoparticles as Methanol Synthesis and Methanol Steam Reforming Catalysts. *J. Catal.* **2012**, *293*, 27–38. [CrossRef]
78. Studt, F.; Sharafutdinov, I.; Abild-Pedersen, F.; Elkjær, C.F.; Hummelshøj, J.S.; Dahl, S.; Chorkendorff, I.; Nørskov, J.K. Discovery of a Ni-Ga Catalyst for Carbon Dioxide Reduction to Methanol. *Nat. Chem.* **2014**, *6*, 320–324. [CrossRef] [PubMed]
79. Shi, Z.; Tan, Q.; Tian, C.; Pan, Y.; Sun, X.; Zhang, J.; Wu, D. CO_2 Hydrogenation to Methanol over Cu-In Intermetallic Catalysts: Effect of Reduction Temperature. *J. Catal.* **2019**, *379*, 78–89. [CrossRef]
80. Martin, O.; Martín, A.J.; Mondelli, C.; Mitchell, S.; Segawa, T.F.; Hauert, R.; Drouilly, C.; Curulla-Ferré, D.; Pérez-Ramírez, J. Indium Oxide as a Superior Catalyst for Methanol Synthesis by CO_2 Hydrogenation. *Angew. Chem. Int. Ed.* **2016**, *55*, 6261–6265. [CrossRef]
81. Wang, J.; Li, G.; Li, Z.; Tang, C.; Feng, Z.; An, H.; Liu, H.; Liu, T.; Li, C. A Highly Selective and Stable ZnO-ZrO_2 Solid Solution Catalyst for CO_2 Hydrogenation to Methanol. *Sci. Adv.* **2017**, *3*, 1701290. [CrossRef]
82. Wang, J.; Tang, C.; Li, G.; Han, Z.; Li, Z.; Liu, H.; Cheng, F.; Li, C. High-Performance M_aZrO_x (M_a = Cd, Ga) Solid-Solution Catalysts for CO_2 Hydrogenation to Methanol. *ACS Catal.* **2019**, *9*, 10253–10259. [CrossRef]
83. Bansode, A.; Urakawa, A. Towards Full One-Pass Conversion of Carbon Dioxide to Methanol and Methanol-Derived Products. *J. Catal.* **2014**, *309*, 66–70. [CrossRef]
84. Bahruji, H.; Bowker, M.; Hutchings, G.; Dimitratos, N.; Wells, P.; Gibson, E.; Jones, W.; Brookes, C.; Morgan, D.; Lalev, G. Pd/ZnO Catalysts for Direct CO_2 hydrogenation to Methanol. *J. Catal.* **2016**, *343*, 133–146. [CrossRef]
85. Dang, S.; Qin, B.; Yang, Y.; Wang, H.; Cai, J.; Han, Y.; Li, S.; Gao, P.; Sun, Y. Rationally Designed Indium Oxide Catalysts for CO_2 Hydrogenation to Methanol with High Activity and Selectivity. *Sci. Adv.* **2020**, *6*, aaz2060. [CrossRef] [PubMed]
86. Angelo, L.; Kobl, K.; Tejada, L.M.M.; Zimmermann, Y.; Parkhomenko, K.; Roger, A.C. Study of CuZn MOx Oxides (M = Al, Zr, Ce, CeZr) for the Catalytic Hydrogenation of CO_2 into Methanol. *Comptes Rendus Chim.* **2015**, *18*, 250–260. [CrossRef]
87. Hu, J.; Yu, L.; Deng, J.; Wang, Y.; Cheng, K.; Ma, C.; Zhang, Q.; Wen, W.; Yu, S.; Pan, Y.; et al. Sulfur Vacancy-Rich MoS_2 as a Catalyst for the Hydrogenation of CO_2 to Methanol. *Nat. Catal.* **2021**, *4*, 242–250. [CrossRef]
88. Wang, L.; Guan, E.; Wang, Y.; Wang, L.; Gong, Z.; Cui, Y.; Meng, X.; Gates, B.C.; Xiao, F.S. Silica Accelerates the Selective Hydrogenation of CO_2 to Methanol on Cobalt Catalysts. *Nat. Commun.* **2020**, *11*, 1033. [CrossRef] [PubMed]
89. Braz, C.G.; Matos, H.A.; Mendes, A.; Rocha, J.F.; Alvim, R.P. Model of an Industrial Reactor for Formaldehyde Production with Catalyst Deactivation. In *Computer Aided Chemical Engineering*; Elsevier: Amsterdam, The Netherlands, 2017; pp. 121–126.
90. Brookes, C.; Bowker, M.; Wells, P. Catalysts for the Selective Oxidation of Methanol. *Catalysts* **2016**, *6*, 92. [CrossRef]
91. Thrane, J.; Mentzel, U.V.; Thorhauge, M.; Høj, M.; Jensen, A.D. A Review and Experimental Revisit of Alternative Catalysts for Selective Oxidation of Methanol to Formaldehyde. *Catalysts* **2021**, *11*, 1329. [CrossRef]

92. Malik, M.I.; Abatzoglou, N.; Achouri, I.E. Methanol to Formaldehyde: An Overview of Surface Studies and Performance of an Iron Molybdate Catalyst. *Catalysts* **2021**, *11*, 893. [CrossRef]
93. Millar, G.J.; Collins, M. Industrial Production of Formaldehyde Using Polycrystalline Silver Catalyst. *Ind. Eng. Chem. Res.* **2017**, *56*, 9247–9265. [CrossRef]
94. Franz, A.W.; Kronemayer, H.; Pfeiffer, D.; Pilz, R.D.; Reuss, G.; Disteldorf, W.; Gamer, A.O.; Hilt, A. Formaldehyde. In *Ullmann's Encyclopedia of Industrial Chemistry*; Wiley-VCH Verlag GmbH & Co. KGaA: Weinheim, Germany, 2016; pp. 1–34.
95. Söderhjelm, E.; House, M.P.; Cruise, N.; Holmberg, J.; Bowker, M.; Bovin, J.-O.; Andersson, A. On the Synergy Effect in MoO_3–$Fe_2(MoO_4)_3$ Catalysts for Methanol Oxidation to Formaldehyde. *Top. Catal.* **2008**, *50*, 145–155. [CrossRef]
96. Andersson, A.; Holmberg, J.; Häggblad, R. Process Improvements in Methanol Oxidation to Formaldehyde: Application and Catalyst Development. *Top. Catal.* **2016**, *59*, 1589–1599. [CrossRef]
97. Hassan, K.H.; Mitchell, P.C.H. Evaluation of Different Methods to Prepare the Fe_2O_3/MoO_3 Catalyst Used for Selective Oxidation of Methanol to Formaldehyde. In *Studies in Surface Science and Catalysis*; Elsevier: Amsterdam, The Netherlands, 2010; pp. 475–478.
98. Soares, A.P.V.; Portela, M.F.; Kiennemann, A.; Hilaire, L. Mechanism of Deactivation of Iron-Molybdate Catalysts Prepared by Coprecipitation and Sol–Gel Techniques in Methanol to Formaldehyde Oxidation. *Chem. Eng. Sci.* **2003**, *58*, 1315–1322. [CrossRef]
99. Beale, A.M.; Jacques, S.D.M.; Sacaliuc-Parvalescu, E.; O'Brien, M.G.; Barnes, P.; Weckhuysen, B.M. An Iron Molybdate Catalyst for Methanol to Formaldehyde Conversion Prepared by a Hydrothermal Method and Its Characterization. *Appl. Catal. A Gen.* **2009**, *363*, 143–152. [CrossRef]
100. Liu, X.; Kong, L.; Liu, C.; Xu, S.; Zhang, D.; Ma, F.; Lu, Z.; Sun, J.; Chen, J. Study on the Formation Process of $MoO_3/Fe_2(MoO_4)_3$ by Mechanochemical Synthesis and Their Catalytic Performance in Methanol to Formaldehyde. *J. Therm. Anal. Calorim.* **2020**, *142*, 1363–1376. [CrossRef]
101. Popov, B.I.; Shkuratova, L.N.; Skorokhova, N.G. Influence of Sodium Salts on the Catalytic Properties of Iron-Molybdenum Oxide Catalysts in the Oxidation of Methanol to Formaldehyde. *React. Kinet. Catal. Lett.* **1975**, *3*, 463–469. [CrossRef]
102. Sanderson, J.R.; Lin, J.J.; Duranleau, R.G.; Yeakey, E.L.; Marquis, E.T. Free Radicals in Organic Synthesis. A Novel Synthesis of Glycerol Based on Ethylene Glycol and Formaldehyde. *J. Org. Chem.* **1988**, *53*, 2859–2861. [CrossRef]
103. Drentm Eit; Mul, W.P.; Ruisch, B.J. Process for the Carbonylation of Formaldehyde. US6376723B2, 23 April 2000.
104. Shattuck, M.T.; Wa, W. Continuous Glycolic Acid Process. US2443482A, 15 June 1948.
105. Bhattacharyya, S.K.; Vir, D. 64 High-Pressure Synthesis of Glycolic Acid from Formaldehyde, Carbon Monoxide, and Water in Presence of Nickel, Cobalt, and Iron Catalysts. In *Advances in Catalysis*; Academic Press: Cambridge, MA, USA, 1957; pp. 625–635.
106. Suzuki, S. Process for the Production of Glycolic Acid and Oxydiacetic Acid. US3911003A, 7 October 1975.
107. Ying, S.; Wang, H.; Liu, Z. Process for Production of Glycolic Acid. WO2009140850A1, 26 November 2009.
108. Zhu, Z.; Kang, G.; Yu, S.; Qin, Y.; Sun, Y.; Cao, Y. Process Intensification in Carbonylation of Formaldehyde with Active and Passive Enhancement Methods. *J. Flow. Chem.* **2020**, *10*, 605–613. [CrossRef]
109. Shi, Q.; Guo, H.; Chen, C.; Hou, B.; Jia, L.; Li, D. Study on the Performance of $CF3SO_3H$ Modified Sulfonic Polymer-Based Catalyst in Formaldehyde Carbonylation Reaction. *J. Fuel Chem. Technol.* **2020**, *48*, 875–882.
110. Cao, X.; Zhang, K.; Wang, Y.; He, P. Boosting the Production of Glycolic Acid from Formaldehyde Carbonylation via the Bifunctional PdO/ZSM-5 Catalyst. *Ind. Eng. Chem. Res.* **2023**, *62*, 17671–17680. [CrossRef]